Vol. 48, No. 2, pp 131-138, 2020
Indian Journal of Soil Conservation

Prioritization of critical soil erosion prone areas in a snow dominated Himalayan basin using remote sensing and GIS

Akram Ahmed[1,*], Ambrish Kumar[2], J.M.S. Tomar[3]

[1]ICAR Research Complex for Eastern Region, ICAR Parisar, Patna, Bihar; [2]College of Agricultural Engineering, Dr Rajendra Prasad Central Agricultural University, Pusa, Samastipur, Bihar; [3]ICAR-Indian Institute of Soil and Water Conservation, 218 Kaulagarh Road, Dehradun.

**Corresponding author:*
E-mail: akrambckv@gmail.com (Akram Ahmed)

ARTICLE INFO

Article history:
Received : September, 2019
Revised : July, 2020
Accepted : August, 2020

Key words:
GIS
Remote Sensing
Soil erosion
USLE
Watersheds

ABSTRACT

Much emphasis is laid these days on the sustainable development of watersheds. Sustainable development relates to fulfilling the demand for a given area with respect to growing demographic pressure without disturbing the ecological balance. Soil loss due to erosion is one of the major components that is affected by human intervention and is required for maintaining ecological balance. In this study, an attempt has been made to prioritize the areas within the Teesta river basin, a sub–basin of Brahmaputra river basin in India according to their soil loss rate using remote sensing (RS) and geographical information system (GIS) techniques. The universal soil loss equation (USLE) was used to quantify soil loss from the study area. The maximum and minimum soil loss from the different sub–basins within the study area was estimated as 41.88 t $ha^{-1}yr^{-1}$ and zero t $ha^{-1}yr^{-1}$, respectively. There are 53 sub–basins identified within the Teesta river basin which are observed to exceed the soil loss rate of 5 t ha^{-1} yr^{-1}. The estimates were correlated with observations of suspended sediment in the river at the catchment outlet. It is concluded that soil erosion resistant management practices are needed for adoption in these areas for their sustainable development.

1. INTRODUCTION

Soil is one of the most important components of the natural system that is required for an environmental balance. From a research point of view, its significance lies in providing food to all living creatures of the earth. Of all the soil layers, the top layer of the soil is most productive as it contains the maximum nutrients. Various factors accelerate the removal of the top soil and make the soil unproductive. Water and wind are the most important factors which play a major role in removing the top soil. Water in the form of rainfall and runoff or overland flow displaces the soil particles from one location to another. Rainfall with high kinetic energy directly hits the soil particles and displaces them. The kinetic energy of falling raindrops is proportional to the rainfall intensity. When the rainfall intensity increases, the amount of displaced soil particles also multiplies. However, the erosion characteristic of soils varies with the soil types. Generally, cohesive soil has a smaller propensity of getting eroded but possesses a tendency of getting transported. Organic matter present in the soil decelerates the rate of soil erosion. It increases the stability of soil particles by forming large soil aggregates. On the other hand, soils having more permeability for moderately high rainfall intensity will produce less runoff as well as soil erosion. The other important factors which influence the soil erosion process are slope degree and length of the sloping land, soil cover, and the land practices adopted for an area. Eroded soil from an area is transported by overland flow, which is finally discharged to a stream. This continuous soil loss from an area reduces the stream depth, and thus increases the extent of flood plain of the stream which may lead to loss of useful land area. Likewise, soil loss also reduces the effective life span of reservoirs. Narayan and Babu (1983) reported that on an average 5334 million tonnes of soil is being eroded in India every year. It has been highlighted that under future climate change scenarios there may be much more soil erosion throughout the world (Amore *et al.,* 2004).

Extensive studies on soil erosion have been undertaken before and a large number of models on soil erosion have been reported by workers, like Wischmeier and Smith (1978); Adinarayana *et al.* (1999), Lal (2001), Shen *et al.* (2003), Lu

et al. (2004). However, the USLE proposed by Wischmeier and Smith (1978) is still extensively used for estimating soil loss at basin–scale (Griffin *et al.,* 1988; Dickinson and Collins, 1998; Jain *et al.,* 2001; Shinde *et al.,* 2010). In many of the soil erosion studies, basin has been divided into a suitable number of grids to study the spatial distribution pattern of soil erosion (Julien and Gonzales del Tanago, 1991; Wilson and Gallant, 1996; Kothyari and Jain, 1997; Onyando *et al.,* 2005; Wu *et al.,* 2005; Dabral *et al.,* 2008; Singh and Panda, 2017). Following the rapid progress in RS and GIS techniques and due to the accuracy and reliability of data obtained from it, a lot of work on soil erosion estimation in GIS environment has been carried out (Renschler *et al.,* 1997; Sidhu *et al.,* 1998; Khan *et al.,* 2001; Sharma *et al.,* 2001; Yoshino and Ishioka, 2005; Pandey *et al.,* 2007; Belayneh *et al.,* 2019; Kumar *et al.,* 2019). Ahmed *et al.* (2017) overlaid USLE model parameters under GIS environment to categorize places in the Gumti basin, Tripura in India under various soil loss classes. They have shown that the soil loss in the basin ranges from 0.03 t ha^{-1} yr^{-1} to 114.08 t $ha^{-1}yr^{-1}$. Kadam *et al.* (2019) estimated the spatial soil erosion susceptibility in 14 sub–watersheds of the Western Ghats of India using RS and GIS techniques. Biswas *et al.* (2019) mapped soil erosion risk prone areas in Karnataka region, Southern India for conservation of natural resources.

The present study was conducted for the Teesta river basin located in eastern Himalayas, which forms a part of the Brahmaputra river basin. The Brahmaputra originates as Tsangpo in Tibet (China). Incidentally, the world's third–highest mountain peak Kangchenjunga (8586 m) is also situated within the study area. So far, there has not yet been any work reported on soil erosion quantification for the Teesta basin. In the present study, RS and GIS techniques were used to estimate the soil erosion from different sub–basins of the Teesta basin using USLE formulation.

2. MATERIALS AND METHODS

Study Area

Teesta is one of the major tributaries of the Brahmaputra river which originates from Sikkim Himalayas at an elevation of 5330 m from above mean sea level (AMSL). Teesta river is internationally significant as it travels through India and flows into Bangladesh. Eventually, the river Teesta meets the Brahmaputra river in Bangladesh. Sikkim has a completely mountainous topography while West Bengal is partly mountainous and partly plain within the present study area (Fig. 1) with a downstream outlet at the Gazaldoba Barrage in West Bengal. The geographical extent of the study area lies between $87^0 59' 24''$E to $88^0 52' 48''$E longitude and $26^0 43' 29''$N to $28^0 7' 40''$N latitude, sprawling over 8735 km^2. The northern part of the study area lies mostly under permanent snow cover. The total length of Teesta river up to the outlet is 214 km and flows for about 172 km in mountainous terrain before emerging into the alluvial plains of West Bengal. Within Bangladesh, it flows for about 124 km before meeting the Brahmaputra. The important tributaries of the Teesta river include Lachungchu, Dikchu, Rongnichu, Rangpochu, Rangit, etc. Stream order of the Teesta river network as shown in Fig. 1 as per Strahler (1957) at the outlet (Gazaldoba Barrage) is found to be five.

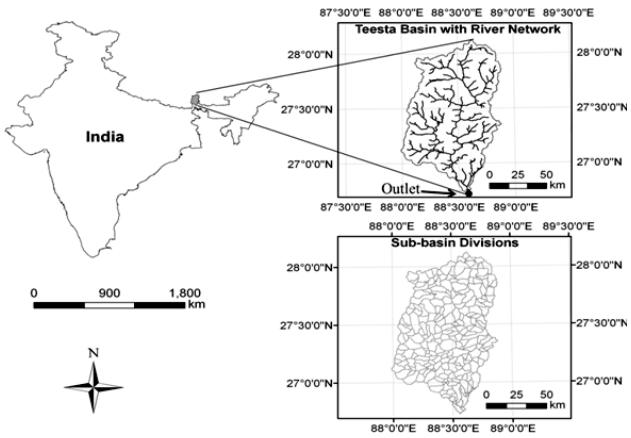

Fig. 1. Index map of Teesta basin, river network and sub-basin divisions of Teesta basin

Methods for Parameter Estimation

The soil loss within the study area was estimated using the USLE. A brief detail of this equation is discussed in this section. Also, the parameters used in the USLE formulation are explained, which have been derived using the GIS software package Arc–Info 9.3.1.

Universal Soil Loss Equation (USLE)

The USLE was first formulated by Wischmeier and Smith (1978) for estimating gross average soil loss rate from small agricultural fields, but it was later applied widely for estimating annual average soil loss in basin scale. However, it includes factors like climate, soil, topography, and land use/land cover (LU/LC) for estimating the annual average soil loss rate from a basin. The USLE is expressed as:

$$A = RKLSCP \quad \ldots(1)$$

Where, A is the average annual gross soil erosion or soil loss rate (t $ha^{-1}yr^{-1}$); R is the rainfall erosivity factor (MJ mm $ha^{-1}hr^{-1}yr^{-1}$); K is the soil erodibility factor (t ha hr $ha^{-1}Mj^{-1}$ mm^{-1}); L is the slope length factor; S is the slope gradient factor; C is the crop cover or crop management factor; and P is the supportive conservation practice factor. All these factors are derived from basic data sources as indicated in the work–flow chart, Fig. 2, alongwith the application methodology.

Rainfall Erosivity Factor (*R*)

Rainfall erosivity factor (R) depends upon kinetic energy of falling raindrops, and kinetic energy is a function of rainfall intensity. Due to the absence of rainfall intensity information for the study area, daily rainfall data was used

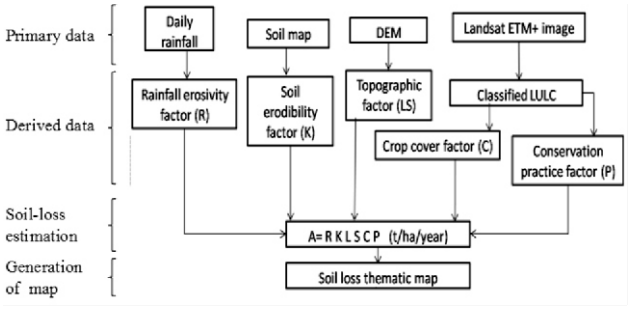

Fig. 2. Flow chart describing the procedure for soil loss estimation from primary data

for estimating *R*. Panigrahi *et al.* (1996) proposed a model for estimating rainfall erosivity factor using daily rainfall data, which expresses rainfall erosivity factor as:

$$R = P^2 (0.00364 \log_{10} P - 0.000062) \quad \ldots(2)$$

Where, *P* is the daily rainfall in mm. The daily rainfall information was downloaded from Asian Precipitation – Highly – Resolved Observational Data Integration towards Evaluation "APHRODITE" (V1003R1 dataset having spatial resolution of 0.25^0) www.chikyu.ac.jp/precip/ was used for rainfall erosivity factor calculation. In total, 18 gridded rainfall stations within or nearby the study area were used. For each station, the daily rainfall data of ten years (1998–2007) was employed. Theissen polygon method in Arc-Info software package was used to produce the continuous thematic domains of the study area that falls under coverage of different rainfall stations.

Soil Erodibility Factor (K)

Soil erodibility is defined as the susceptibility of the soil particles against soil erosion. Experimentally, soil erodibility factor was estimated using regression analysis which depends on fractional amounts of clay, sand, very fine sand and silt particle, organic matter content, and soil texture and permeability. The equation is given as (Das, 2010):

$$K = 2.8 \times 10^{-7} \times M^{1.14} \times (12 - a) + 4.3 \times 10^{-3} \times (b - 2) + 3.3 \times 10^{-3} \times (c - 3) \quad \ldots(3)$$

Where, *M* is the particle size parameter [(% silt + % fine sand) (100– % clay)]; *a* is the % organic matter; *b* is the soil structure code (very fine granular, 1; fine granular, 2; medium or course granular, 3; blocky, platy or massive, 4); and, *c* is the soil permeability class (rapid, 1; moderate rapid, 2; moderate, 3; slow to moderate, 4; slow, 5; very slow, 6) (Das, 2010). The soil map along with different soil properties of the study area were collected from National Bureau of Soil Survey and Landuse Planning (NBSS& LUP), Nagpur. There are four major soil groups identified over the study area *i.e.* rock, sandy soil, sandy loam and silt loam. The *K* factor was calculated using eq. 3 using different soil parameters, and thematic vector map of *K* factor was prepared using Arc-Info software package.

Topographic Factor (LS)

Overland flow carries the eroded soil particles down the slope. Soil loss is proportional to the length of slope (*L*). The concentration of the overland flow increases with the increase in slope length. On the other hand, when the steepness of the slope increases, it increases the splash rate. Increase in gradient of slope (*S*) increases the velocity of overland flow, which enhances the eroding as well as the transporting power of overland flow down a slope. Soil and Water Assessment Tool (SWAT) (Neitsch *et al.,* 2005) in Arc-Info environment, which predicts the impact of land management practices on runoff, sediment yield and agricultural chemical yields in large complex basins with varying soils, land use and management conditions, was used here. However, use of SWAT was restricted in this study only for delineation of Teesta basin and generation of sub–basin parameters using the digital elevation model (DEM). The sub–basin parameters calculated using SWAT include sub–basin identity number, area, slope, slope length, perimeter etc. Shuttle Radar Topographic Mission (SRTM) DEM data (Fig. 3a) (www.srtm.csi.cgiar.org/SELECTION/inputCoord.asp) having spatial resolution of 90 m was used for calculation of slope length and steepness of slope. From the attribute table of the sub–basins generated by the SWAT model, slope length and steepness of the slope was obtained for each sub–basin. As the USLE is developed for a unit plot having a length of 22.13 m and nine percent slope, the slope length and steepness of the slope of sub–basins is to be converted into slope length and slope steepness factor to fit into USLE equation. The slope length factor can be written as:

$$L = (L_p / 22.13)^m \quad \ldots(4)$$

Where, L_p is the actual length of slope and *m* is equal to 0.5 when slope is greater than and equal to 5%, 0.4 for 4% and 0.3 for less than and equal to 3% (Das, 2010). The slope gradient factor (*S*) can be calculated as (Wischmeier and Smith, 1978):

$$S = (0.43 + 0.3s + 0.043s^2) / 6.613 \quad \ldots(5)$$

Where, *S* is the slope of the sub–basin in %. The calculated slope length and gradient factor value using eq's 4 and 5 for each sub–basin was used to prepare a thematic vector map using Arc-info software package.

Crop Cover Factor (C)

Vegetative cover dissipates the kinetic energy of the falling rain drops. More the canopy cover, more will be the dissipation of kinetic energy of the rainfall, and consequently less the soil erosion. Canopy cover reduces the diameter of the raindrops and affects the distribution of the rainfall. After hitting the canopy, the rain falls to the ground in the form of throughfall. The energy of the throughfall depends on the height of the canopy. RS and GIS is best way to identify and estimate the spatial variation of the vegeta-

tive cover and other land uses. Cloud–free satellite images of Landsat Enhanced Thematic Mapper Plus (ETM+) for path/row 139/41 of 26th December, 2000 having spatial resolution of 30 m, downloaded from United States Geological Service's (USGS) Earthexplorer website (www.earthexplorer.usgs.gov/) was used for LU/LC classification of the study area. The downloaded ETM+ satellite images are registered with the help of toposheets having scale of 1:250000 downloaded from Perry–Castañeda Library (www.lib.utexas.edu/maps/ams/india/). The LU/LC map over the study area helps in calculating the *C* values for different land uses.

Conservation Practice Factor (P)

Cultivation practiced along the slope causes maximum soil erosion. To cultivate land in steep slope, certain land practices are adopted to reduce soil erosion. The practices include contouring, strip cropping, contour strip cropping, bench terracing etc. These practices reduce the slope length as well as steepness of slope. The predominant land practice adopted in agricultural areas within the study domain are bench terracing in sloping areas and row cropping in plain areas. The *P* factor value corresponding to each land use categories was edited in Arc-info software package to generate thematic map of *P* factor of the study area.

3. RESULTS AND DISCUSSION

Landuse and Land Cover Pattern

Maximum Likelihood Classification method in Earth Resources Data Analysis System (ERDAS) software package was employed to ETM+ satellite image of the year 2000 for LU/LC classification. Eight predominant land use classes (Fig. 3g) were identified within the study area *i.e.* water, natural vegetation, snow, rock, settlement, river bank, agriculture, and barren land. Within the study area, the natural vegetation class was found to contain mostly shrubs and trees. However, it is extremely difficult to distinguish these two categories from the available coarse resolution satellite image of ETM+. Hence, areas having shrubs and trees were considered under the common LU/LC category *i.e.* natural vegetation. The area which came under the flood plains of the river was designated as 'river bank' in the classified image and those having scattered patches of vegetation were classified as 'barren land'. The agricultural area was divided into two categories *i.e.* terrace agriculture and plain agriculture. Terrace agriculture is adopted in steeply sloping areas whereas plain agriculture is practiced in flat areas. The area covered by each land use is shown in Table 1. For accuracy assessment of the classified image, producer's, user's, and overall accuracy were calculated along with kappa statistics. The overall accuracy and kappa coefficient of the LU/LC image was calculated as 85.31 and 0.82, respectively.

Rainfall Erosivity Factor (R) Estimation

Eq. 2 was used for calculation of *R* for each gridded rainfall station. The value of *R* ranged from 0 to 1177 MJ mm $ha^{-1}hr^{-1}yr^{-1}$. The area located in the northern part of the Teesta river basin is covered with permanent snow cover throughout the year. It is assumed that during the occurrence of snowfall, it has a very minute impact on soil causes negligible soil displacement. Therefore, *R* value for snow covered area was assumed zero. Area falling under high rainfall zone, located in the middle and bottom part of the Teesta river basin, has high *R* value. The spatial variation of *R* value is as shown in Fig. 3b.

Soil Erodibility Factor (K) Estimation

Soil erodibility factor calculated using eq. 3 varied from 0 to 0.11 over the study area (Fig. 3d). Since in the upland northern part of the Teesta basin, the sub–basins are under permanent snow cover, and soils are mostly rocky (Fig. 3c); the *K* value for those areas was assigned zero. Among the soil present in the study area, the sandy loam soil has comparatively a higher *K* value. The middle and lower sub–basins, generally having sandy loam soil cover has higher *K* values.

Topographic Factor (LS) Estimation

The Teesta river basin has a completely mountainous topography, except for some portion in the lower valley on the south. The DEM of the study area indicated that the elevation within the basin varies from 98 m to 8509 m above mean sea level (AMSL). The maximum and minimum slopes of the sub–basins are 74% and 1%, respectively whereas the average slope is approximately 49%. The maximum, minimum, and average slope lengths are 122 m, 9 m, and 17 m, respectively. Out of 251 sub–basins, 242 sub–basins were found to have slopes more than 10% and for such high values of the slope, LS factor (eq's 4 and 5) were seen to be high amongst the sub–basins. The maximum and minimum value of the LS factor ranged from 54 to 0.27. Fig. 3e presents the variation of LS value throughout the basin. For most of the sub–basins, the value of LS varied between 10 to 20.

Crop Cover Factor (C) Estimation

The classified LU/LC raster data generated from raw satellite image was divided into 80311 polygon domains using skeletonisation and vector extraction technique (Gold,

Table: 1
Areal coverage of different LU/LC classes

Land use/Land cover	Area (km^2)	% Area
Water	24.78	0.28
Natural vegetation	4177.12	47.82
Snow	2167.90	24.82
Rock	1057.02	12.10
Settlement	109.81	1.26
River bank	27.16	0.31
Agriculture	1140.06	13.05
Barren land	31.48	0.36
Total	8735	100

1999) in Arc-Info software. Each polygon contained only a single LU/LC among classified eight LU/LC. The spatial distribution of *C*, a factor directly dependent upon the land cover, is shown in Fig. 3g. The *C* factor value was assigned to each polygon according to the LU/LC type. The main crops in the mountainous region of the study area are rice, wheat, maize, barley, pulses, potato, orange, and tea and in the plains, rice and tea are cultivated. Crop cover factor values of woodland, terraced agricultural land, plain agricultural land, barren land, settlement, river bank, snow area, water, and rocky area were assigned as 0.01, 0.35, 0.28, 0.5, 0.002, 0.50, 1, 1, and 1, respectively (Das, 2010; Shinde *et al.,* 2010). In the mountainous region, the crop cover factor among crops varies 0.25 to 0.4. Therefore, the average *C* value for crop–lands of mountainous region was assigned as 0.35 whereas crop cover factor in crop–lands of plain area was assigned as 0.28. Natural vegetation has the lowest values of *C* whereas water, snow and rock have the highest *C* value *i.e.* 1.

Conservation Practice Factor (P) Estimation

Conservation practice factor (*P*) was taken as 0.28 for bench terracing and 0.6 for row cropping (Debral *et al.,* 2008). The value of *P* for vegetation, snow, water, barren land, settlement, rock, and river bank was assigned as 0.8, 1, 1, 0.7, 1, 1, and 0.7, respectively (Das, 2010). In the attribute table of the polygon domains of LU/LC in Arc-Info software, the value of *P* for different LU/LC was assigned. The variation of the factor *P* over the study area is shown in Fig. 3h. Fig. 3h clearly shows that terrace agriculture is practiced in the central portion of the basin whereas row crop cultivation is practiced in the plain lands. About 38.36% of the Teesta river basin has *P* value equal to one.

Average Annual Soil Loss (A) Estimation and Validation

The thematic vector map of each component of USLE, except the topographic factor map of sub–basins, was overlaid in Arc-Info which resulted in 80311 polygon domains (generated previously from LU/LC raster data) having information about all USLE components except topographic factor. These USLE factors (R, K, C, and P) corresponding to each polygon domain multiplied with each other resulted in soil loss from those polygons per unit topographic factor. The soil losses (per unit topographic factor) from polygon domains inside a particular sub–basin were summed up to get soil loss per unit topographic factor from that particular sub–basin. Likewise, soil loss per unit topographic factor from each sub–basin was estimated. Topographic factor

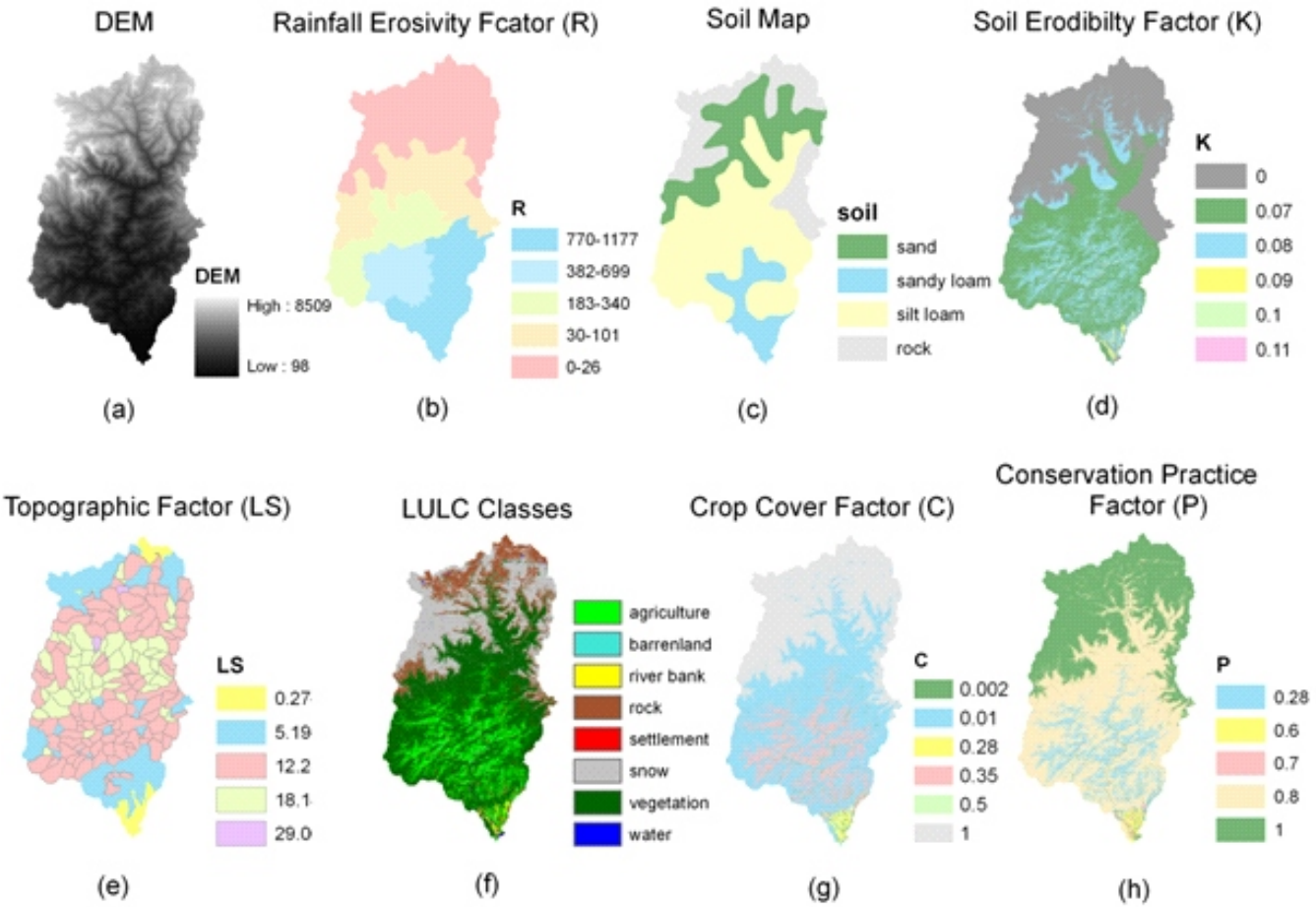

Fig. 3. Thematic layers of DEM, R, soil map, K, LS, LULC, C, and P

(LS) of each sub–basin calculated previously using the SWAT model, multiplied with soil loss per unit topographic factor calculated in previous step resulted in average annual soil loss from each sub–basin (Fig. 4).

Soil loss rate from sub–basins was found to range from 0 to 41.88 t $ha^{-1}yr^{-1}$. It may be noted that this finding matches with those of similar researches carried out on different Himalayan regions. Dhruba (1997) estimated similar soil loss results in the Likhu Khola sub–basin of Nepalese Himalayas (just to the west of the Sikkim Himalayas). In similar topographic scenarios in Kashmir Himalayas situated in the northern part of India, Sheikh *et al*. (2011) found soil loss ranges from 0 to 61 t $ha^{-1}yr^{-1}$. Pandey *et al.* (2009) found soil loss rates varying from 0 to 57 t $ha^{-1}yr^{-1}$ in the Dikrong river basin in north-eastern India. In the present study, the sub–basins having soil loss less than 0.5 t $ha^{-1}yr^{-1}$ were seen mostly to fall under or nearby to the snow covered area. The low value of soil loss in snow covered area is attributed to the low value of *R* and *K* factors. The number of sub–basins that come under each soil loss category is shown in Table 2. Maximum number sub–basins *i.e.* 125 came under the negligible soil loss category followed by slight (59 number), moderate (38 number), normal (14 number), high (12 in number), very high (2), and severe (number 1) soil loss category. It was observed that barren lands contribute to the highest soil loss compared to the other LU/LC classes. Sub–basin number 184 was estimated to have the maximum soil loss rate of 41.88 t $ha^{-1}yr^{-1}$ due to the presence of more fractional barren land area compared to other sub–basins. Sub–basin categorized under negligible, normal, and slight

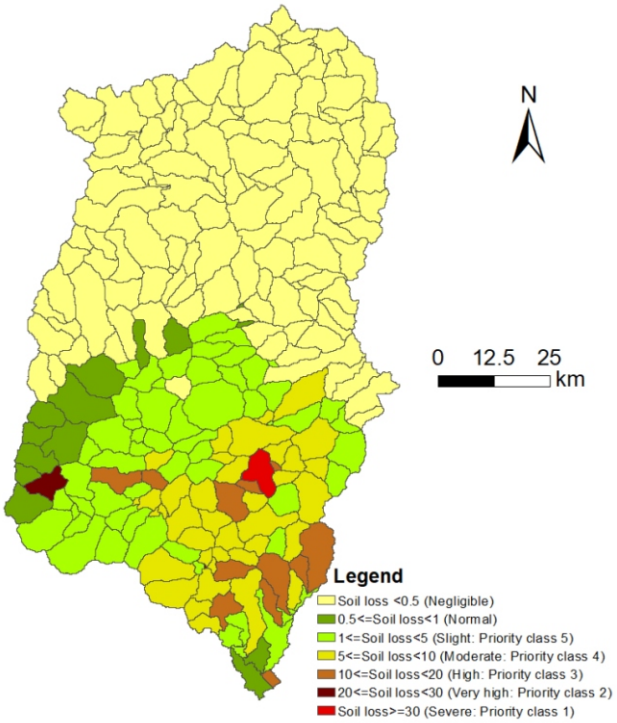

Fig. 4. Sub-basin wise soil loss (t $ha^{-1}yr^{-1}$) map

Table: 2
Soil loss category classification

Amount of soil loss (t $ha^{-1}yr^{-1}$)	Number of sub-basin	Category
Soil loss < 0.5	125	Negligible
0.5< = soil loss < 1	14	Normal
1< = soil loss < 5	59	Slight
5< = soil loss < 10	38	Moderate
10< = soil loss < 20	12	High a
20< = soil loss < 30	2	Very high
Soil loss > = 30	1	Severe

soil loss categories contribute less sediment to the Teesta river network. Therefore, sub–basins are to be prioritized to treat them with suitable soil conservation measures to limit the soil loss of those sub–basins to normal. The location of the sub–basins to treat them in priority is shown in Fig. 4. The sub–basins with the highest soil loss are kept under priority class 1 followed by sub–basins under priority class 2, priority class 3, and so on. No watershed treatment measures are required at present for the sub–basins with soil loss under the negligible and normal category. Suitable watershed treatment measures include increasing vegetation cover through afforestation (particularly in barren lands), contour trenching combined with the vegetative barrier, construction of gabions as well as check dams across channels, etc.

Since it is difficult to obtain field data for validating the estimated soil loss from sub–basins directly, the observed sediment yield data at the Reshi and Khanitar river gauging stations were used as an indirect means of validation. This data, procured from Central Water Commission (CWC), Gangtok, India, pertains to two catchments (catchments generated with downstream outlets at Reshi and Khanitar stations, respectively), having areas 1273 km^2 and 5488 km^2, respectively, as shown in Fig. 5. The gross soil loss from these catchments was calculated by summing up the soil loss from sub–basins, which fall inside the catchments.

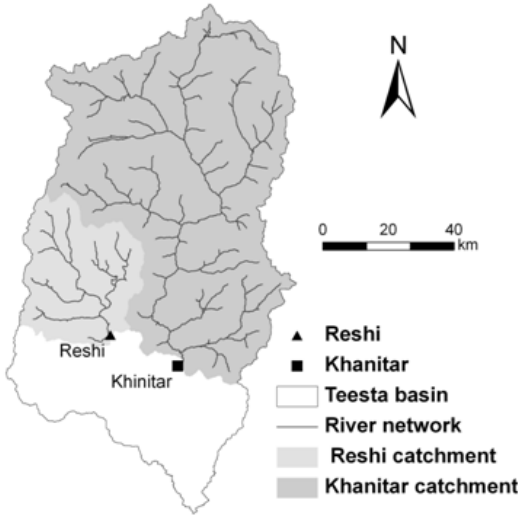

Fig. 5. Location of Reshi and Khanitar river gauging stations in study area and their catchments

The values of sediment yield at these two stations were estimated using sediment delivery ratio (SDR) which is defined as the observed sediment yield as a fraction of the gross soil erosion (*A*) from a catchment. The values of average SDR were computed as 0.0320 and 0.0149 using observed sediment yield and gross estimated soil loss data of five years (2003 to 2007) for Reshi and Khanitar catchments, respectively which, when multiplied with corresponding gross soil loss rate estimated at these two stations, provided an estimation for sediment yield (Table 3). The observed and estimated sediment yield at Reshi and Khanitar stations as well as annual average rainfall over the catchments were compared for 5 years in Table 4. Results indicated that for each year, the estimated sediment yield is generally greater (except for the years 2004 and 2006 for Reshi; 2004 and 2005 for Khanitar, respectively) than the observed sediment yield. One reason for this may be due to the fact that the observed data obtained from the CWC is a measure of only the suspended load, whereas the estimated sediment load invariably includes all forms of sediment load including bed load that may be conveyed by the river. On the other hand, there are situations of river bank erosion and landslides that increase the material transported by the river which, though not taken into account in this approach, is related to the physically observed data. However, correlating with such additional loads would require information on erosion and landslides, which are not used at present.

A wide variation of observed sediment yield may also be noted which is likely to have occurred as a result of the variation of rainfall erosivity factor over the basin. An increase in rainfall intensity as well as the amount, increases soil loss. Estimated sediment yield was maximum both in Reshi as well as Khanitar catchment in 2003 probably due to the extreme rainfall that had occurred on that year in comparison to other years (Fig. 6).

4. CONCLUSIONS

RS and GIS techniques were used in this study to map the spatial distribution of soil loss from the Teesta river basin. Teesta river deposits a huge amount of sediment in the downstream plains each year, eroded from the upstream mountainous catchment. Hence, it is of rather immediate necessity to identify the areas which are prone to heavy soil erosion in the Teesta river catchment. In this study, RS and GIS techniques were used for categorizing the sub–basins

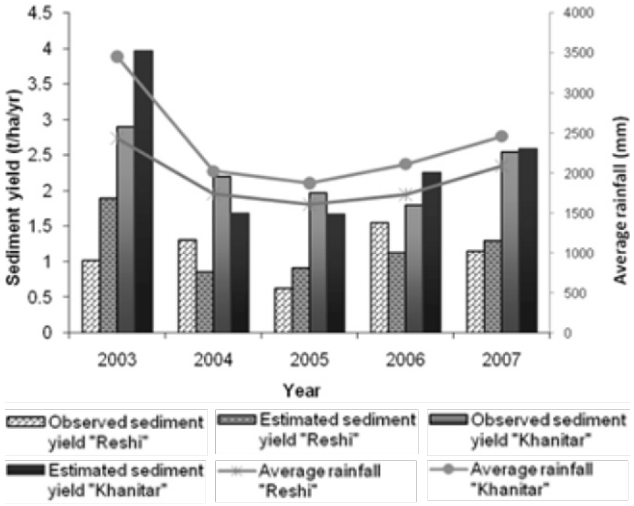

Fig. 6. Comparison of sediment yield and average rainfall corresponding to Reshi and Khanitar catchments

Table: 3
Average sediment delivery ratio for Reshi and Khanitar catchments

Year	Reshi catchment				Khanitar catchment			
	Observed sediment yield ($t\ ha^{-1}yr^{-1}$)	Estimated soil loss ($t\ ha^{-1}yr^{-1}$)	Sediment delivery ratio	Average rainfall (mm)	Observed sediment yield ($t\ ha^{-1}yr^{-1}$)	Estimated soil loss ($t\ ha^{-1}yr^{-1}$)	Sediment delivery ratio	Average rainfall (mm)
2003	1.011	59.251	0.0171	0.0320	2.905	266.998	0.0109	0.0149
2004	1.313	26.615	0.0493		2.199	113.250	0.0194	
2005	0.619	28.629	0.0216		1.973	112.472	0.0175	
2006	1.551	35.406	0.0438		1.802	151.739	0.0119	
2007	1.147	40.671	0.0282		2.539	173.946	0.0146	

Table: 4
Comparison of observed and estimated sediment yield

Year	Reshi catchment			Khanitar catchment		
	Observed sediment yield ($t\ ha^{-1}yr^{-1}$)	Esimated soil loss ($t\ ha^{-1}yr^{-1}$)	Average sediment delivery ratio	Observed sediment yield ($t\ ha^{-1}yr^{-1}$)	Estimated soil loss ($t\ ha^{-1}yr^{-1}$)	Average sediment delivery ratio
2003	1.011	1.891	2435.5	2.905	3.968	3457.0
2004	1.313	0.849	1744.8	2.199	1.683	2025.3
2005	0.619	0.914	1611.5	1.973	1.671	1875.0
2006	1.551	1.130	1737.8	1.802	2.255	2114.8
2007	1.147	1.298	2089.5	2.539	2.585	2461.5

according to their soil erosion rate. It was found that barren land contributes more to soil loss as compared to other LU/LC classes. Therefore, those sub–basins having more fractional barren lands contribute more soil loss. There are about 53 sub–basins that fall under the severe, very high, high, and moderate soil loss category within the Teesta river basin where intensive soil conservation measures like trenching, afforestation, building check dams and concrete structures, etc. may have to be adopted immediately.

ACKNOWLEDGMENTS

The authors are thankful to Central Water Commission, Ministry of Water resources, India and National Bureau of Soil Survey and Landuse Planning (NBSS&LUP), Nagpur, Indian Council of Agricultural Research, India for providing different hydrological data and soil map of Sikkim and West Bengal, respectively for this research.

REFERENCES

Adinarayana, J., Rao, K.G., Krishna, N.R., Venkatachalam, P. and Suri, J.K. 1999. A rule–based soil erosion model for a hilly catchment. *Catena*, 37: 309–318.

Ahmed, I., Pan, N.D., Debnath, J. and Bhowmik, M. 2017. An assessment to prioritise the critical erosion–prone sub–watersheds for soil conservation in the Gumti basin of Tripura, North–East India. *Environ. Monit. Assess.,* 189(11): 600.

Amore, E., Modica, C., Nearing, M.A. and Santoro, V.C. 2004. Scale effect in USLE and WEPP application for soil erosion computation from three Sicilian basins. *J. Hydrol.,* 293(1–4): 100–114.

Belayneh, M., Yirgu, T. and Tsegaye, D. 2019. Potential soil erosion estimation and area prioritization for better conservation planning in Gumara watershed using RUSLE and GIS techniques'. *Environ. Syst. Res.,* 8(1): 20.

Dabral, P.P., Baithuri, N. and Pandey, A. 2008. Soil erosion assessment in a hilly catchment of North Eastern India using USLE, GIS and remote sensing. *Water Resour. Manag.,* 22: 1783–1798.

Das, G. 2010. Hydrology and soil conservation engineering: including watershed management. Phi Learning, New Delhi.

Dhruba, P.S. 1997. Assessment of soil erosion in the Nepalese Himalaya, a case study in Likhu Khola valley, middle mountain region. Land Husbandry, Oxford and IBH Publishing Co. Pvt. Ltd, 2(1): 59–80.

Dickinson, A. and Collins, R. 1998. Predicting erosion and sediment yield at the catchment scale. CAB International, pp 317–342.

Gold, C.M. 1999. *Crust and anti–crust: A one–step boundary and skeleton extraction algorithm.* In: Proc. 15th Annual ACM Symposium Computational Geomorphology, pp 189–196.

Griffin, M.L., Beasley, D.B., Fletcher, J.J. and Foster, G.R. 1988. Estimating soil loss on topographically non–uniform field and farm units. *J. Soil Water Conserv.,* 43: 326–331.

Biswas, H., Raizada, A., Kumar, S., Mandal, D., Srinivas, S., Hedge, R. and Mishra, P.K. 2019. Soil erosion risk mapping for natural resource conservation planning in Karnataka region, southern India. *Indian J. Soil Cons.,* 47(1): 14-20.

Jain, S.K., Kumar, S. and Varghese, J. 2001. Estimation of soil erosion for a Himalayan watershed using GIS technique. *Water Resour. Manag.*, 15: 41–54.

Julien, P.Y. and Del Tanago, M.G. 1991. Spatially varied soil erosion under different climates. *Hydrolog. Sci. J.,* 36(6): 511–524

Kadam, A.K., Jaweed, T.H., Kale, S.S., Umrikar, B.N. and Sankhua, R.N. 2019. Identification of erosion–prone areas using modified morphometric prioritization method and sediment production rate: A remote sensing and GIS approach. *Geomatics, Nat. Hazards Risk,* 10(1): 986–1006.

Khan, M.A., Gupta, V.P. and Moharanam, P.C. 2001. Watershed prioritization using remote sensing and geographical information system: A case study from Guhiya, India. *J. Arid Environ.,* 49: 465–475.

Kothyari, U.C. and Jain, S.K. 1997. Sediment yield estimation using GIS. *Hydrolog. Sci. J.,* 42(6): 833–843.

Kumar, M., Singh, P.K., Kumar, R., Mittal, H.K., Yadav, K.K. and Garg, K.S. 2019. Planning of conservation measures using remote sensing and geographical information system in micro-watershed. *Indian J. Soil Cons.,* 47(1): 37-44.

Lal, R. 2001. Soil degradation by erosion. *Land Degrad. Dev.,* 12: 519–539.

Lu, D., Li, G., Valladares, G.S. and Batistella, M. 2004. Mapping soil erosion risk in Rondônia, Brazilian Amazonia: using RUSLE, Remote Sensing and GIS. *Land Degrad. Dev.,* 15: 499–512.

Narayan, D.V.V. and Babu, R. 1983. Estimation of soil erosion in India. *J. Irrig. Drain. E.,* 109(4): 419–431.

Neitsch, S.L., Arnold, J.G., Kiniry, J.R. and Williams, J.R. 2005. Soil and water assessment tool theoretical decumnetation, Blackland Research Center, Texas.

Onyando, J.O., Kisoyan, P. and Chemelil, M.C. 2005. Estimation of potential soil erosion for river Perkerra catchment in Kenya. *Water Resour. Manag.,* 19: 133–143.

Pandey, A., Chowdary, V.M. and Mal, B.C. 2007. Identification of critical erosion prone areas in the small agricultural watershed using USLE, GIS and remote sensing. *Water Resour. Manag.,* 21: 729–746.

Pandey, A., Mathur, A., Mishra, S.K. and Mal, B.C. 2009. Soil erosion modeling of a Himalayan watershed using RS and GIS. *Environ. Earth Sci.,* 59: 399–410.

Panigrahi, B., Senapati, P.C. and Behera, B.P. 1996. Development of erosion index model from daily rainfall data. *J. Appl. Hydrol.,* 9 (1–2): 17–22.

Renschler. C., Diekkruger, B. and Mannaerts, C. 1997. Regionalization in surface runoff and soil erosion risk evaluation, in regionalization of hydrology. IAHS–AISH publication, 254: 233–241.

Sharma, J.C., Prasad, J., Saha, S.K. and Pande, L.M. 2001. Watershed prioritization based on sediment yield index in eastern part of Doon Valley using RS and GIS. *Indian J. Soil Water Cons.*, 29(1): 7–13.

Sheikh, A.H., Palria, S. and Alam, A. 2011. Integration of GIS and universal soil loss equation (USLE) for soil loss estimation in a Himalayan watershed. *Rec. Res. Sci. Tech.,* 3(3): 51–57.

Shen, D., Ma, A.N., Lin, H., Nie, X.H., Mao, S.J., Zhang, B. and Shi, J.J. 2003. A new approach for simulating water erosion on hillslopes. *Int. J. Remote Sens.,* 24: 2819–2835.

Shinde, V., Tiwari, K.N. and Singh, M. 2010. Prioritization of micro watersheds on the basis of soil erosion hazard using remote sensing and geographic information system. *Int. J. Water Resour. Environ. Engg.,* 2(3): 130–136.

Sidhu, G.S., Das, T.H., Singh, R.S., Sharma, R.K. and Ravishankar, T. 1998. Remote sensing and GIS techniques for prioritization of watershed: A case study in upper Mackkund watershed, Andhra Pradesh. *Indian J. Soil Water Cons.*, 2(3): 71–75.

Singh, G. and Panda, R.K. 2017. Grid–cell based assessment of soil erosion potential for identification of critical erosion prone areas using USLE, GIS and remote sensing: A case study in the Kapgari watershed, India. *Int. Soil Water Conserv. Res.,* 5(3): 202–211.

Strahler, A.N. 1957. Quantitative analysis of watershed geomorphology. *Eos. Trans. AGU,* 38(6): 913–920.

Wilson, J.P. and Gallant, J.C. 1996. EROS: A grid–based program for estimating spatially distributed erosion indices. *Comput. Geosci.,* 22(7): 707–712.

Wischmeier, W.H. and Smith, D.D. 1978. Predicting rainfall erosion losses. USDA Agricultural Research Services Handbook 537, USDA, Washington, DC, 57p.

Wu, S., Li, J. and Huang, G. 2005. An evaluation of grid size uncertainty in empirical soil loss modelling with digital elevation models. *Env. Model Asses.,* 10: 33–42.

Yoshino, K. and Ishioka, Y. 2005. Guidelines for soil conservation towards integrated basin management for sustainable development: A new approach based on the assessment of soil loss risk using remote sensing and GIS. *Paddy Water Environ.,* 3: 235–247.